International Journal of Academic and Applied Research (IJAAR)
ISSN: 2000-005X
Vol. 2 Issue 11, November – 2018, Pages: 12-26

A Mathematical Study of MHD Mixed Convection Channel Flow of Nanofluid

***V. Ananthaswamy[1], M. Subha[2] and S. Kaveri[3]**
[1]Department of Mathematics, The Madura College, Madurai, Tamilnadu, India
[2]Department of Mathematics, MSNPM Women's College, Poovanthi, Tamilnadu, India
[3]M. Phil., Mathematics, The Madura College, Madurai, Tamilnadu, India
*Corresponding author e-mail: ananthu9777@rediffmail.com

Abstract: *The purpose of this article is to study and analyse the convective flow of nanofluid. The dimensionless entropy generation equation is obtained by solving the reduced momentum and energy equations. The momentum and energy equations are reduced to a system of ordinary differential equations by a similarity method. The Homotopy analysis method (HAM) is used to solve the resulting system of ordinary differential equations. The HAM is a valid mathematical tool for most of non-linear problems in science and engineering. The main purpose of the paper is to study the effects of Reynolds number, dimensionless temperature difference, Brinkman number, Hartmann number and other physical parameters on the entropy generation. These results are analysed and discussed.*

Keywords : Channel flow; Mixed convection; Nanofluid; Entropy generation; Bejan number; Homotopy analysis method.

1. INTRODUCTION

The history of fluid flow is very old, one of the early studies is the work of Leonardo Da Vinci's which gave rapid advanced to the study of fluids mechanics about 500 years ago, but earlier than this time; prehistoric relics of irrigation canals have shown that the study of fluid behaviour were much more available by the time of ancient Egyptian (Nakayama and Boucher, 1999). Several centuries ago Johan and Daniel began more modern understanding of fluids motion known as Bernoulli's equation. Since then, many researchers have done numerous work on fluid mechanics.

The study of fluid flow and heat transfer in a vertical porous channel have been given considerable attention in the past few decades due to its wide applications in areas such as the design of cooling systems for electronic devices, chemical processingequipment, microelectronic cooling and solar energy (Jamalabadi et al., 2015). Numerous authors who conducted investigations on such flow include: Mutuku-Njaneand Makinde (2013) who investigated the combined effects of buoyancy force and Navier slip on MHD flow of a Nanofluid over a convectively heated vertical porousplate and submitted that increase in Grashof number decreases the fluid velocity. Int he work of Jamalabadi et al. (2015), in which optimal design of Magnetohydrodynamic mixed convection flow in a vertical channel with slip boundary conditions and thermal radiation effects was analysed by using an entropy generation minimization method. It was concluded that Grashof numbers to Reynolds number ratio are better for maximizing the energy of the system. Adesanya and Falade (2015) presented the study on thermodynamic analysis for a third grade fluid through a vertical channel with internal heat generation, among the submissions was that increase in the Grashof number depletes the energy level of the thermal system. In addition, heat transfer dominates the channel with increase in Grashof number. Also, Sharma etal. (2014) investigated radiative and free convective effects on MHD flow through a porous medium with periodic wall temperature and heat generation or absorption with the conclusion that increase in Grashof number increases the skin-friction coefficient at the wall.

2. Mathematical formulation of the problem

Consider the unsteady, incompressible Cu-water nanofluid in a vertical channel having permeable walls as shown in Fig. 1. The fluid is flowed at constant pressure gradient and an external uniform magnetic field is applied perpendicular to the plates. It is presumed that the fluid is injected uniformly into the channel at the fixed lower plate whereas the uniform fluid suction occurs at the moving upper plate. A transverse magnetic field with strength B0 is applied parallel to the Y-axis. The magnetic Reynolds number and the induced electric field are assumed to be small and negligible. The channel width is denoted by h with uniform temperature T0 at Y=0 and temperature T1 at Y= h such that T0<T1. The volume fraction of the Cu-nanoparticles in the base fluid is taken to be from 0 to 10% (i.e. Φ = 0 to 0.1) and assumed to have been mixed homogeneously with the base fluid under laboratory condition thus we have a single phase flow.

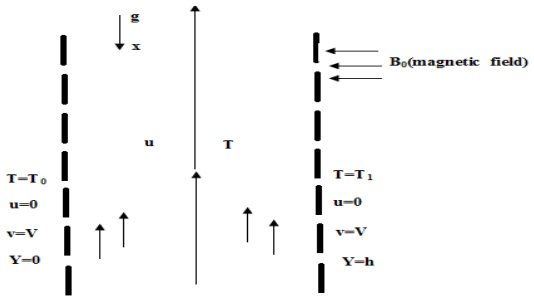

Fig.1:Schematic diagram of the problem

Using the Boussinesq approximation, the governing equations for the momentum and energy balance can be expressed as [7,8,11,16,7,19];

$$-V\frac{du}{dy}+\beta_{nf}g(T-T_0)-\frac{1}{\rho_{nf}}\frac{dP}{dx}+\frac{\mu_{nf}}{\rho_{nf}}\frac{d^2u}{dy^2}-\frac{\sigma_{nf}B_0{}^2u}{\rho_{nf}}=0 \quad (1)$$

$$-(\rho C_P)_{nf}V\frac{dT}{dy}+k_{nf}\frac{d^2T}{dy^2}+\mu_{nf}\left(\frac{du}{dy}\right)^2+\sigma_{nf}B_0{}^2u^2=0 \quad (2)$$

$$E_g=\frac{k_{nf}}{T_0{}^2}\left(\frac{dT}{dy}\right)^2+\frac{\mu_{nf}}{T_0}\left(\frac{du}{dy}\right)^2+\frac{\sigma_{nf}B_0{}^2u^2}{T_0} \quad (3)$$

With the following boundary conditions

$$u(0)=u(h)=0$$
$$T(0)=T_0,\ T(h)=T_1 \quad (4)$$

where u is the axial velocity, P is the pressure, x is the axial distance, is the nanofluid density, is the nanofluiddynamic viscosity, is the nanofluid specific heat capacity at constant pressure, is the nanofluid thermal conductivity, is the entropy generation rate, T is the nanofluid temperature, is the nanofluid electrical conductivity, g is the gravitational acceleration and is the nanofluid thermal expansion coefficient. In the eqns. (1), (2) and (3) the *Cu*-water nanofluid thermophysical properties are given by [17-21]

$$\rho_{nf}=(1-\Phi)\rho_{bf}+\Phi\rho_P,\quad (\rho C_P)_{nf}=(1-\Phi)(\rho C_P)_{bf}+\Phi(\rho C_P)_P,$$

$$(\rho\beta)_{nf}=(1-\Phi)(\rho\beta)_{bf}+\Phi(\rho\beta)_P,\frac{k_{nf}}{k_{bf}}=\frac{\left(k_P+2k_{bf}\right)-2\Phi\left(k_{bf}-k_P\right)}{\left(k_P+2k_{bf}\right)+\Phi\left(k_{bf}-k_P\right)}, \quad (5)$$

$$\sigma_{nf}=\sigma_{bf}\left[1+\frac{3(\gamma-1)\Phi}{(\gamma+2)-(\gamma-1)\Phi}\right],\ \gamma=\frac{\sigma_P}{\sigma_{bf}},\ \mu_{nf}=\frac{\mu_{bf}}{(1-\Phi)^{2.5}}$$

Table:1 Thermophysical properties of water and *Cu* nanoparticles [17-21]

Materials	$\rho(kg/m^3)$	$C_P(J/kgK)$	$k(W/mK)$	$\sigma(S/m)$	$\beta X10^5(K^{-1})$
Pure water	997.1	4179	0.613	$5.5X10^{-6}$	21
Copper (cu)	8933	385	401	$59.6X10^6$	1.67

here ρ_{bf} is the base fluid density, ρ_P is the nanoparticles density, μ_{bf} is the base fluid dynamic viscosity, k_{bf} is the basefluid thermal conductivity, k_P is the nanoparticles thermal conductivity, β_{bf} is the base fluid thermal expansion coefficient, β_P is the nanoparticles thermal expansion coefficient, C_{Pbf} is the base fluid specific heat capacity, C_{PP} is the nanoparticles specific heat capacity, σ_{bf} is the base fluid electrical conductivity and σ_P is the nanoparticles electrical conductivity. Introducing

the following dimensionless parameters and variables,

$$W=\frac{uh}{\upsilon_{bf}},\ Gr=\frac{g\beta_{bf}\left(T_1-T_0\right)h^3}{\upsilon^2{}_{bf}},\ \Pr=\frac{\left(\mu C_P\right)_{bf}}{k_{bf}},\ Ha^2=\frac{\sigma_{bf}B_0{}^2h^2}{\mu_{bf}},$$

$$y=\frac{Y}{h},\ L=\frac{d\overline{P}}{dX},\ Br=\frac{\mu_{bf}\upsilon^2{}_{bf}}{k_{bf}\left(T_1-T_0\right)h^2},\ A1=Q\left[1+\frac{3(\gamma-1)\Phi}{(\gamma+2)-(\gamma-1)\Phi}\right],$$

$$Q=(1-\Phi)^{2.5},\ \theta=\frac{T-T_0}{T_1-T_0},M=\frac{\left(k_P+2k_{bf}\right)+\Phi\left(k_{bf}-k_P\right)}{\left(k_P+2k_{bf}\right)-2\Phi\left(k_{bf}-k_P\right)},$$

$$\overline{P}=\frac{Ph^2\rho_{bf}}{\mu^2{}_{bf}},\ \mathrm{Re}=\frac{Vh}{\upsilon_{bf}},\ Ec=\frac{\upsilon^2{}_{bf}}{C_{Pbf}\left(T_1-T_0\right)h^2},A3=Q\left[1-\Phi+\Phi\frac{(\rho\beta)_P}{(\rho\beta)_{bf}}\right],$$

$$A4=\frac{M}{Q},\ A5=M\left[1+\frac{3(\gamma-1)\Phi}{(\gamma+2)-(\gamma-1)\Phi}\right],\ Ns=\frac{h^2E_g{T_0}^2}{k_{bf}\left(T_1-T_0\right)^2},$$

$$A2=Q\left[1-\Phi+\Phi\frac{\rho_P}{\rho_{bf}}\right],\ A6=M\left[1-\Phi+\Phi\frac{\left(\rho C_P\right)_P}{\left(\rho C_P\right)_{bf}}\right], \tag{6}$$

$$X=\frac{x}{h},\ \upsilon_{bf}=\frac{\mu_{bf}}{\rho_{bf}},\ \gamma=\frac{\sigma_P}{\sigma_{bf}}$$

For a given set of parameter values, the reactive convection flow evolves in time until a steady state condition is attained whenever this happens, then the equations becomes

$$\frac{d^2w}{dy^2}=A2\,\mathrm{Re}\frac{dw}{dy}+A1\,Ha^2\,w-A3\,Gr\,\theta-Q\,L \tag{7}$$

$$\frac{d^2\theta}{dy^2}=A6\,\Pr\mathrm{Re}\frac{d\theta}{dy}-A4\,Ec\,\Pr\left(\frac{dw}{dy}\right)^2-A5\,Ec\,\Pr\,Ha^2\,w^2 \tag{8}$$

The corresponding boundary conditions are as follows:

$$w(0)=0,\ \theta(0)=0$$
$$w(1)=0,\ \theta(1)=1 \tag{9}$$

Table: 2 Numerical values of the constants A1 to A6 can be determine as follows:

Constant / Φ	*A1*	*A2*	*A3*	*A4*	*A5*	*A6*	*Q*	*M*
0	1	1	1	1	1	1	1	1
0.05	1.02	1.23	0.87	0.98	1	0.85	0.88	0.86
0.1	1.02	1.38	0.75	0.97	1	0.74	0.77	0.75

By assumption, the exact solution of the eqn.(7) for the velocity of fluid is possible under this constant viscosity scenario and we obtain

$$w(y) = \frac{Q\,L\,A1\,A2\,A3\,Gr}{2}\left(y - y^2\right) \quad (10)$$

In many engineering and industrial processes, entropy production destroys the available energy in the system. It is therefore imperative to determine the rate of entropy generation in a system, in order to optimize energy in the system for efficient operation in the system. The convection process in a channel is inherently irreversible and this causes continuous entropy generation. Using the eqn. (6), the dimensionless form of local entropy generation rate in an eqn. (3) is given as follows:

$$N_S = \frac{1}{M}\left(\frac{d\theta}{dy}\right)^2 + \frac{Br}{\Omega Q}\left[\left(\frac{dw}{dy}\right)^2 + A1\,Ha^2 w^2\right] \quad (1)$$

where $\Omega = \dfrac{T_w - T_0}{T_0}$ denotes the temperature difference parameter. The Bejan number and the entropy generation rate are defined as follows:

$$Be = \frac{N_1}{N_S} = \frac{1}{1+\phi} \quad (12)$$

and

$$N_S = N_1 + N_2 \quad (13)$$

where

$$N_1 = \frac{1}{M}\left(\frac{d\theta}{dy}\right)^2 \quad (14)$$

$$N_2 = \frac{Br}{\Omega Q}\left[\left(\frac{dw}{dy}\right)^2 + A1\,Ha^2 w^2\right] \quad (15)$$

$$\lambda = \frac{N_2}{N_1} \quad (16)$$

Here N_1 denotes heat transfer irreversibility due to heat transfer, N_2 denote fluid friction and magnetic field irreversibility, Φ denotes irreversibility ratio. The Bejan number as shown in an eqn.(12) has a range of $0 \le Be \le 1$. If $Be = 0$, then the irreversibility is dominated by the combined effects of fluid friction and magnetic fields, but if $Be = 1$, then the irreversibility due to heat transfer dominates the flow system by the virtue of finite temperature differences.

3 Solution of the non-linear boundary value problems using the Homotopy analysis method

In this paper an analytic tool for nonlinear problems, namely the Homotopy analysis method (HAM) by Liao [22], is employed as our basic concept to solve the nonlinear differential eqns., (3) and (4). The Homotopy analysis method is based on a music concept in topology, i.e. Homotopy by Hilton [23] which is widely applied in numerical techniques as in [24–27]. Unlike perturbation techniques [28-30], the Homotopy analysis method is independent of small/large parameters. Unlike all other reported perturbation and non-perturbation techniques such as the artificial small parameter method, the expansion method and Adomian decomposition method , the Homotopy analysis method provides us with a simple way to adjust and control the convergence region and rate of approximation series. The Homotopy analysis method has been successfully applied to many nonlinear problems such as viscous flows, heat transfer, nonlinear oscillations, nonlinear water waves, Thomas Fermi's atom model, etc.

In particular, by means of the Homotopy analysis method, the author Liao [33] gave a drag

formula for a sphere in a uniform stream, which agrees well with experimental results in a considerably larger region of Reynolds number than those of all reported analytic drag formulas. These successful applications of the Homotopy analysis method verify its validity for nonlinear problems in science and engineering. The Homogony analysis method contains the auxiliary parameter *h*, which provides us with a simple way to adjust and control convergence region of solution series. The approximate analytical expressions of the velocity and temperature profiles using Homotopy analysis method are as follows:

$$w(y)=\frac{QLA1A2A3Gr}{2}\left(y-y^2\right)-h\left[\begin{array}{l}\frac{QLA1A2^2A3Gr\,\mathrm{Re}}{2}\left(\frac{y^2}{2}-\frac{y^3}{3}\right)\\+\frac{QLA1^2A2A3Gr\,Ha^2}{2}\left(\frac{y^3}{6}-\frac{y^4}{12}\right)\\-\left(\frac{-1}{2}\frac{y^2}{e^f-1}+\frac{e^{f,y}}{f^2\left(e^f-1\right)}\right)A3Gr-\frac{QLy^2}{2}\\+t_1y+t_2\end{array}\right] \tag{17}$$

$$\theta(y)=C_1+C_2e^{f.y}-h\left[\begin{array}{l}\left(\frac{e^{f.y}}{A4\,A5\,Ec\left(e^f-1\right)}\right)\\-\left(\frac{A1^2A2^2A3^2A4\,Ec\,\mathrm{Pr}\,Q^2L^2Gr^2}{192}\right).\left(1-2y^4\right)\\-\left(\frac{A1^2A2^2A3^2A5\,Ec\,\mathrm{Pr}\,Q^2L^2Gr^2Ha^2}{4}\right).\\\left(\frac{y^6}{30}-\frac{y^5}{10}+\frac{y^4}{12}\right)+t_3y+t_4\end{array}\right] \tag{18}$$

where

$$f=A4\,A5\,A6\,\mathrm{Pr}\,\mathrm{Re}\,Ec \tag{19}$$

$$c_1=\frac{-1}{e^f-1} \tag{20}$$

$$c_2=\frac{1}{e^f-1} \tag{21}$$

$$t_1 = \left(\frac{-A3\,Gr}{f^2\left(e^f - 1\right)} \right) - \left(\frac{A1^2\,A2\,A3\,Gr\,Q\,L\,Ha^2}{24} \right) - \left(\frac{A2^2\,A1\,A3\,Gr\,Q\,L\,\mathrm{Re}}{12} \right)$$

$$+ \left(\frac{-1}{2\left(e^f - 1\right)} + \frac{e^f}{f^2\left(e^f - 1\right)} \right) A3\,Gr + \left(\frac{Ql}{2} \right) \qquad (22)$$

$$t_2 = \frac{A3\,Gr}{f^2\left(e^f - 1\right)} \qquad (23)$$

$$t_3 = \left[\frac{-e^f}{f^2\left(e^f - 1\right)} \right] + \left(\frac{A1^2\,A2^2\,A3^2\,Gr^2\,Q^2\,L^2\,Ha^2\,Ec\,\mathrm{Pr}\,A5}{240} \right) + \frac{1}{A4\,A5\,Ec\left(e^f - 1\right)} \qquad (24)$$

$$t_4 = \left(\frac{A1^2\,A2^2\,A3^2\,Gr^2\,Q^2\,L^2\,Ec\,\mathrm{Pr}\,A4}{192} \right) - \left(\frac{1}{A4\,A5\,Ec\left(e^f - 1\right)} \right) \qquad (25)$$

4. Results and discussion

Figure 1 shows the schematic diagram of the problem. Fig.2 (a)-(e) represents the dimensionless transverse coordinate versus dimensionless fluid velocity. From Fig. 2 (a), it is clear that when irreversibility ratio increases the corresponding dimensionless fluid velocity profiles decreases in some fixed values of the other parameters $L, \mathrm{Pr}, \mathrm{Re}, Ec, Ha, Gr$ and h. From Fig. 2 (b), it is observed that when the Reynolds number increases the corresponding dimensionless fluid velocity profiles decreases in some fixed values of the other parameters. From Fig.2 (c), it is inferred that when the Grashof number increases the corresponding dimensionless fluid velocity profiles increases in some fixed values of the other parameters. From Fig. 2 (d), it is depict that when the Hartmann number increases the corresponding dimensionless fluid velocity profiles decreases in some fixed values of the other parameters. From Fig. 2 (e), it is noted that when the Eckert number increases the corresponding dimensionless fluid velocity profiles increases in some fixed values of the other parameters.

Figure 3(a)-(d) are representing the dimensionless transverse coordinate versus Dimensionless fluid temperature profiles. From Fig.3 (a), it is inferred that the irreversibility ratio increases fluid temperature profiles increases in some fixed values of the other parameters $L, \mathrm{Pr}, \mathrm{Re}, Ec, Ha, Gr$ and h. From Fig. 3 (b), it is observed that when the Reynolds number increases the corresponding dimensionless fluid temperature profiles decreases in some fixed values of the other parameters. From Fig. 3 (c), it is clear that when the Grashof number increases the corresponding dimensionless fluid temperature profiles increases in some fixed values of the other parameters. From Fig. 3 (d), it is depict that when the Hartmann number increases the corresponding dimensionless fluid temperature profiles decreases in some fixed values of the other parameters.

Figure 4 (a)-(c) are represent the Entropy generation rate versus dimensionless transverse coordinate. From Fig.4 (a) it is inferred that the irreversibility ratio increases entropy generation rate increases in some fixed values of the other parameters $L, \mathrm{Pr}, \mathrm{Re}, Ec, Ha, Gr, Br\Omega^{-1}$ and h.

From Fig. 4 (b), it is observed that when the Reynolds number increases the corresponding entropy generation rate decreases in some fixed values of the other parameters. From Fig. 4 (c), it is noted that when the $Br\Omega^{-1}$ increases the corresponding entropy generation rate increases in some fixed values of the other parameters.

Figure 5 (a)-(c) are represent the dimensionless transverse coordinate versus Bejan number. From Fig.5 (a) it is inferred that the irreversibility ratio increases Bejan number increases in some fixed values of the other parameters $L, \Pr, \mathrm{Re}, Ec, Ha, Gr, Br\Omega^{-1}$ and h. From Fig. 5 (b), it is observed that when the Reynolds number increases the corresponding Bejan number decreases in some fixed values of the other parameters. From Fig. 5 (c), it is noted that when the $Br\Omega^{-1}$ increases the corresponding Bejan number decreases in some fixed values of the other parameters.

(a)

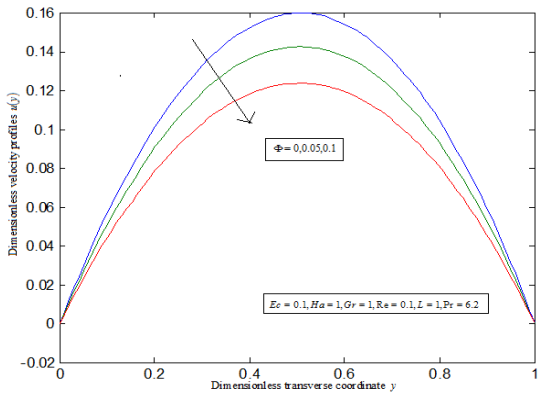

(b)

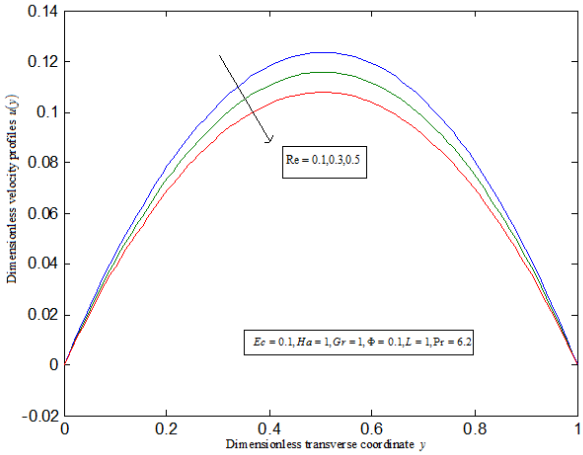

(c)

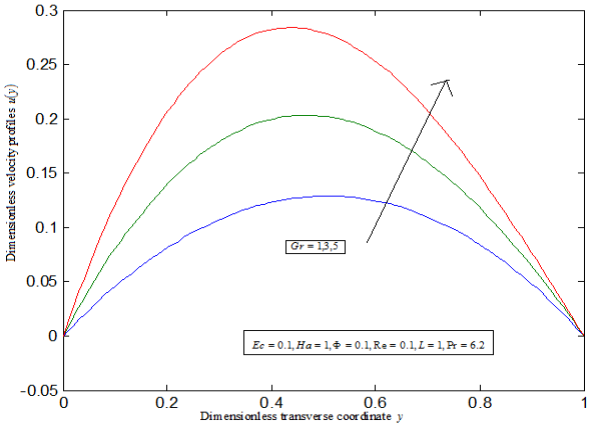

(d)

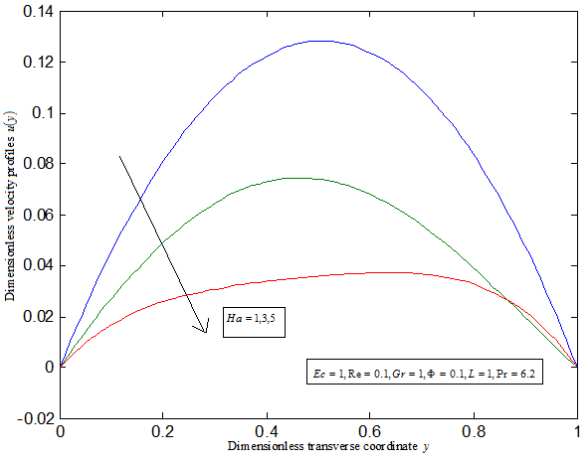

(e)

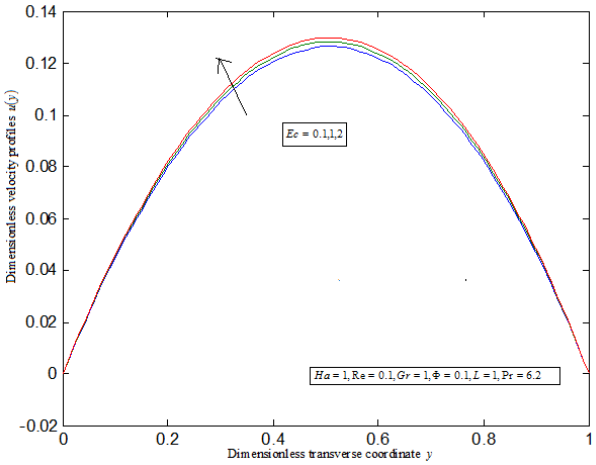

Fig. 2 (a)-(e): Dimensionless fluid velocity profiles $w(y)$ versus dimensionless transverse coordinate (y). The curves are plotted using the eqn. (17) for various values of the dimensionless parameter $\Pr, L$ and in some fixed values of the other dimensionless parameters, when

$(a)\, Ec, Ha, Gr, \mathrm{Re}, \Phi = 0, h = -0.20,\ Ec, Ha, Gr, \mathrm{Re}, \Phi = 0.05, h = -0.15,$

$Ec, Ha, Gr, \mathrm{Re}, \Phi = 0.1, h = -0.16$

$(b)\, Ec, Ha, Gr, \mathrm{Re} = 0.1, \Phi, h = -0.16\ ,\quad Ec, Ha, Gr, \mathrm{Re} = 0.3, \Phi, h = -0.10,$

$Ec, Ha, Gr, \mathrm{Re} = 0.5, \Phi, h = -0.04$

$(c)\, Ec, Ha, Gr = 1, \mathrm{Re}, \Phi, h = -0.20\ ,\ Ec, Ha, Gr = 3, \mathrm{Re}, \Phi, h = 0.52,\ Ec, Ha, Gr = 5, \mathrm{Re}, \Phi, h = 0.855$

$(d)\, Ec, Ha = 1, Gr, \mathrm{Re}, \Phi, h = -0.20,\ Ec, Ha = 3, Gr, \mathrm{Re}, \Phi, h = 0.72,\ Ec, Ha = 5, Gr, \mathrm{Re}, \Phi, h = -0.49$

$(e)\, Ec = 0.1, Ha, Gr, \mathrm{Re}, \Phi, h = -0.18,\ Ec = 1, Ha, Gr, \mathrm{Re}, \Phi, h = -0.20,\ Ec = 2, Ha, Gr, \mathrm{Re}, \Phi, h = -0.22$

(a)

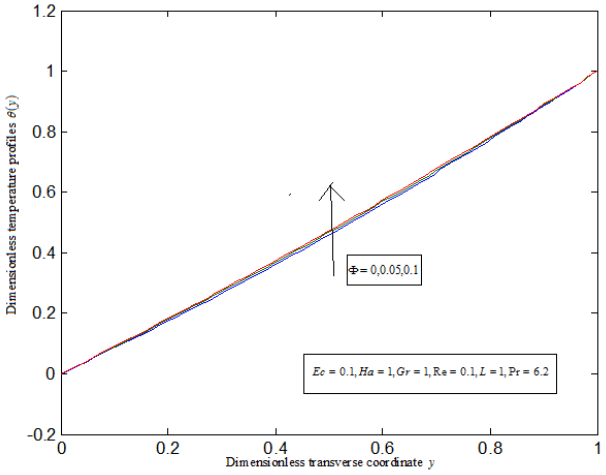

(b)

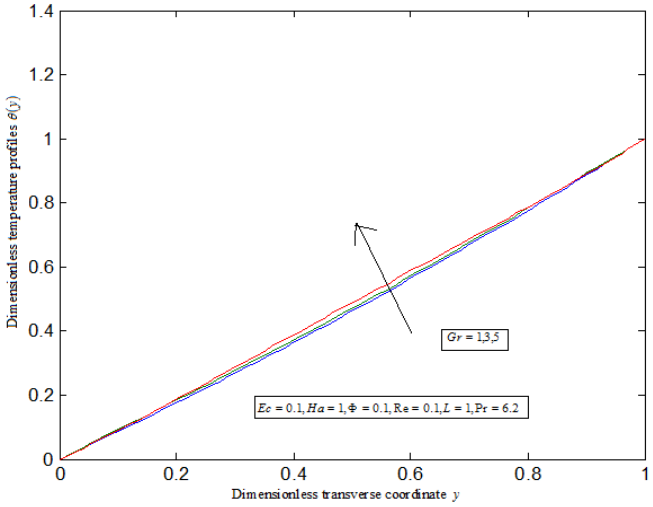

(d)

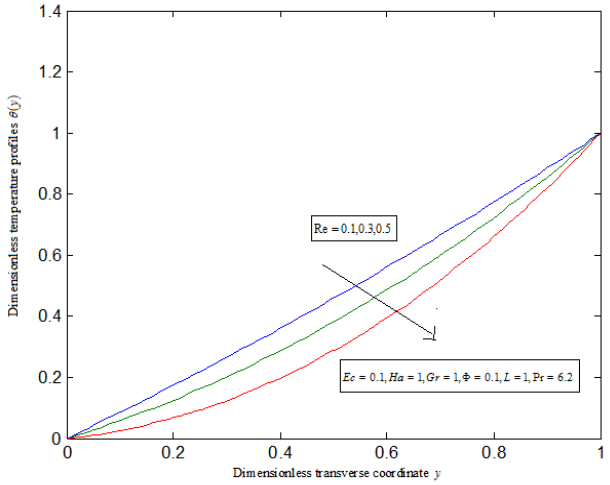

(c)

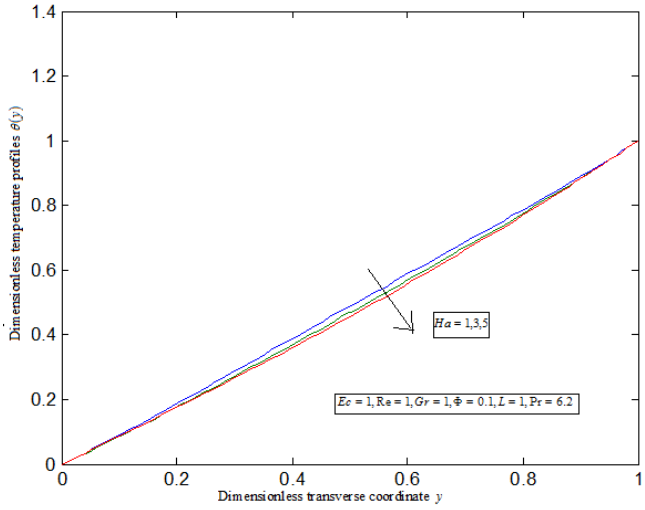

Fig. 3 (a)-(d) : Dimensionless fluid temperature profiles $\theta(y)$ versus dimensionless transverse coordinate (y). The curves are plotted using the eqn. (18) for various values of the dimensionless parameter $\Pr, L$ and in some fixed values of the other dimensionless parameters, when

$(a)\, Ec, Ha, Gr, \mathrm{Re}, \Phi = 0, h = -0.45,\ Ec, Ha, Gr, \mathrm{Re}, \Phi = 0.05, h = -0.43,$
$Ec, Ha, Gr, \mathrm{Re}, \Phi = 0.1, h = -0.40$

$(b)\, Ec, Ha, Gr, \mathrm{Re} = 0.1, \Phi, h = -0.65\ ,\quad Ec, Ha, Gr, \mathrm{Re} = 0.3, \Phi, h = -0.60,$
$Ec, Ha, Gr, \mathrm{Re} = 0.5, \Phi, h = -0.65$

$(c)\, Ec, Ha, Gr = 1, \mathrm{Re}, \Phi, h = -0.59\ ,\ Ec, Ha, Gr = 3, \mathrm{Re}, \Phi, h = -0.72,\ Ec, Ha, Gr = 5, \mathrm{Re}, \Phi, h = 0.55$

$(d)\, Ec, Ha = 1, Gr, \mathrm{Re}, \Phi, h = 0.80\ ,\quad Ec, Ha = 3, Gr, \mathrm{Re}, \Phi, h = -0.7,\quad Ec, Ha = 5, Gr, \mathrm{Re}, \Phi, h = 0.01$

(a)

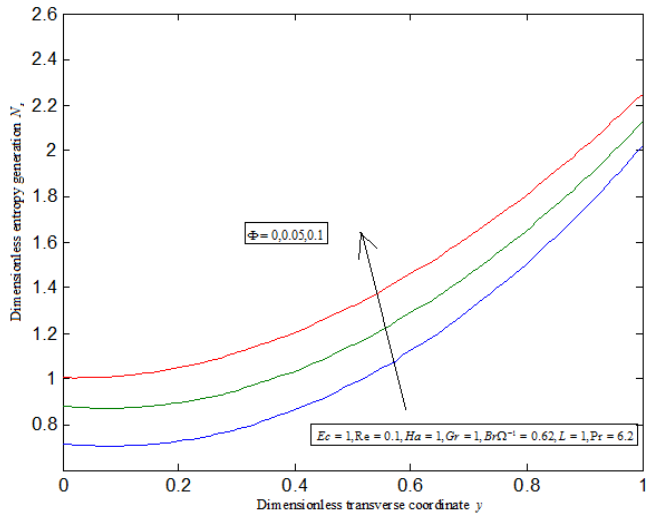

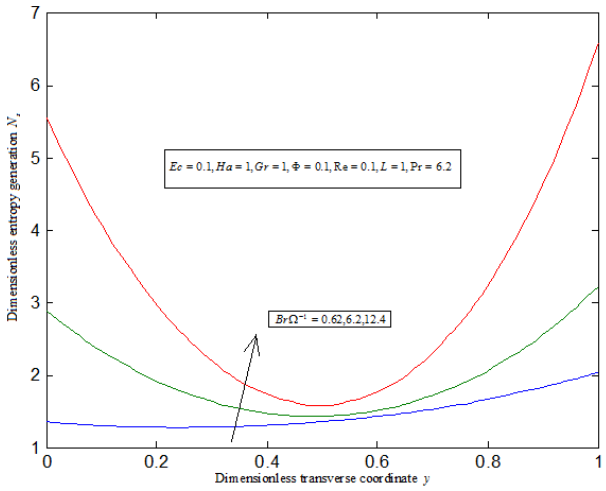

(b)

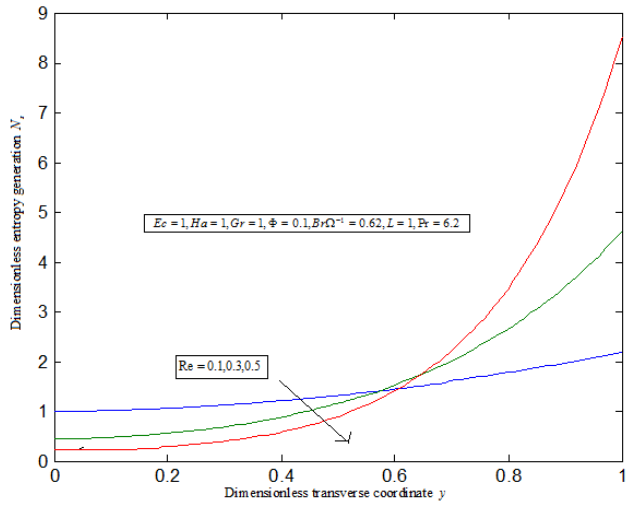

(c)

Fig. 4 (a)-(c) : Dimensionless entropy generation rate *Ns* versus dimensionless transverse coordinate (y).The curves are plotted using the eqn. (11) for various values of the dimensionless parameter Pr, L and in some fixed values of the other dimensionless parameters, when

$(a)\, Ec, Ha, Gr, \mathrm{Re}, Br\Omega^{-1}, \Phi = 0, h = -0.10,\ Ec, Ha, Gr, Br\Omega^{-1}, \mathrm{Re}, \Phi = 0.05, h = -0.10,$

$Ec, Ha, Gr, \mathrm{Re}, Br\Omega^{-1}, \Phi = 0.1, h = -0.11$

$(b)\, Ec, Ha, Gr, Br\Omega^{-1}, \mathrm{Re} = 0.1, \Phi, h = -0.03\ ,\quad Ec, Ha, Gr, Br\Omega^{-1}, \mathrm{Re} = 0.3, \Phi, h = -0.03,$

$Ec, Ha, Gr, Br\Omega^{-1}, \mathrm{Re} = 0.5, \Phi, h = -0.01$

$(c)\, Ec, Ha, Gr = 1, Br\Omega^{-1} = 0.62\,\mathrm{Re}, \Phi, h = -0.45\ ,\ Ec, Ha, Gr = 3, \mathrm{Re}, Br\Omega^{-1} = 6.2\Phi, h = -0.10,$

$Ec, Ha, Gr = 5, \mathrm{Re}, \Phi, h = -0.25$

(a)

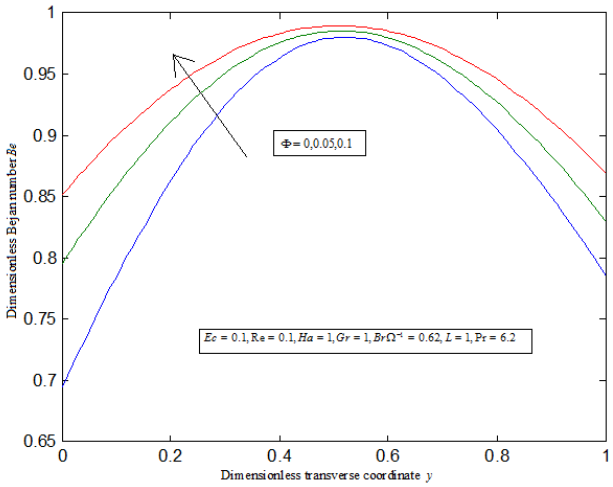

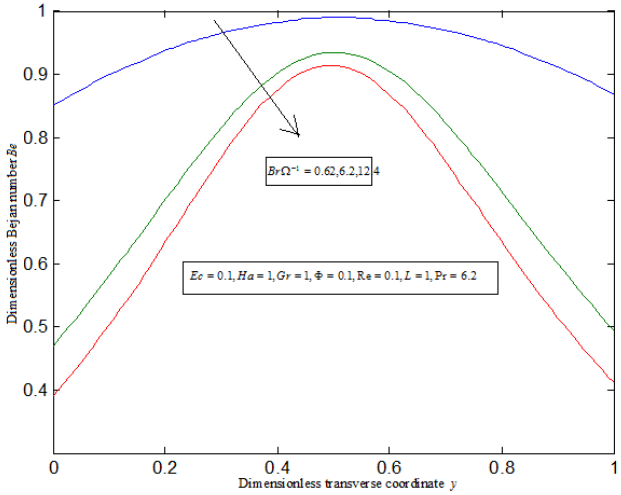

(b)

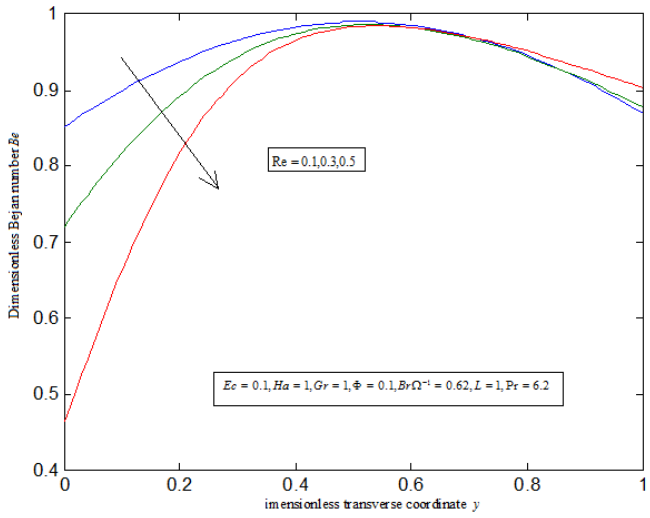

(c)

Fig. 5 (a)-(c) : Dimensionless Bejan number Be versus dimensionless transverse coordinate (y).The curves are plotted using the eqn. (12) for various values of the dimensionless parameter Pr, L and in some fixed values of the other dimensionless parameters, when

$(a)\, Ec, Ha, Gr, \mathrm{Re}, Br\Omega^{-1}, \Phi = 0, h = -0.50,\ Ec, Ha, Gr, Br\Omega^{-1}, \mathrm{Re}, \Phi = 0.05, h = -0.28,$

$Ec, Ha, Gr, \mathrm{Re}, Br\Omega^{-1}, \Phi = 0.1, h = -0.20$

$(b)\, Ec, Ha, Gr, Br\Omega^{-1}, \mathrm{Re} = 0.1, \Phi, h = -0.20\ ,\quad Ec, Ha, Gr, Br\Omega^{-1}, \mathrm{Re} = 0.3, \Phi, h = -0.35,$

$Ec, Ha, Gr, Br\Omega^{-1}, \mathrm{Re} = 0.5, \Phi, h = -0.43$

$(c)\, Ec, Ha, Gr = 1, Br\Omega^{-1} = 0.62\, \mathrm{Re}, \Phi, h = -0.20\ ,\quad Ec, Ha, Gr = 3, \mathrm{Re}, Br\Omega^{-1} = 6.2\Phi, h = -0.02,$

$Ec, Ha, Gr = 5, \mathrm{Re}, \Phi, h = -0.11$

5. Conclusions

A mathematical study is carried out for the entropy generation rate in hydromagnetic mixed convection flow of Cu-Water nanofluid through a channel with permeable wall. The velocity and the temperature profiles are obtained graphically and analytically with the Homotopy analysis method. We can also derive the analytical expressions for the skin friction, Nusselt number, entropy generation number with the Bejan number. The analytical results were obtained through this paper demonstrates that the optimal design and the efficient performance of a flow system involving nanofluid or a thermally designed system can be improved by choosing the appropriate values of the physical parameters. The Homotopy analysis method (HAM) contains the convergence control parameter *h*, so that it can be extend to solve the other MHD fluid flow problems in other engineering and sciences.

References

[1] O.D. Makinde and M.S. Tshehla, "Effects of convective heating on entropy Generation rate in a channel, Global Journal of Pure and Applied Mathematics, Volume 13, number 9 (2017):4851-4867.

[2] S. O. Adesanya, and J. A.Falade, Thermodynamics analysis of hydromagnetic third-grade fluid flow through a channel filled with porous medium. Alexandria Engineering Journal,57(2015): 615-622 .

[3] M. A. Jamalabadi, Park, J. H.and Lee, C. Y. Optimal design of magnetohytrodynamic mixed convection flow in a vertical channel with slip boundary conditions and thermal radiation effects by using an entropy generation minimization method.Entropy,17 (2015): 866- 881.

[4] W.N. Mutuku-Njane, and O.D. makinde, Combined effects of buoyancy force and Navier slip on MHD floe of a nanofluid over a convectively heated vertical porous plate. The specific world journal,(2013): 1-8.

[5] Y.Nakayama, and R.F. Boucher. Introduction to fluid mechanics. John wiley and son Ins., (1999).

[6] P.R. Sharma, K. Sharma, K. and T. Mehta, Radiative and free convective effects on MHD Flow through a porous medium with periodic wall temperature and heat generation or absorption. International journal of mathematical archive, 5(9) (2014): 119-128.

[7] O.D. Makinde, I. L. Animasaun, Bioconvection in MHD nanofluid flow with nonlinear thermal radiation and quartic autocatalysis chemical reaction past an upper surface of a paraboloid of revolution. International Journal of Thermal Sciences, 109 (2016): 159-171.

[8] S. M. Aminossadati, A. Raisi, B. Ghasemi, Effects of magnetic field on nanofluid forced convection in a partially heated microchannel. Int. J Non-Linear Mech, 46 (2011): 1373–1382.

[9] M. J. Uddin, W.A. Khan, A. I. Md. Ismail, Scaling group transformation for MHD boundary layer slip flow of a nanofluid over a convectively heated stretching sheet with heat generation. Mathematical problems in Engineering, 2012.

[10] A. Bejan, A study of entropy generation in fundamental convective heat transfer. J. Heat Transf. 101(1979), 718-725.

[11]L. C. Woods, Thermodynamics of Fluid Systems. Oxford University Press, Oxford, UK; 1975.

[12] M.H. Mkwizu, O.D. Makinde: Entropy generation in a variable viscosity channel

flow of nanofluid with convective cooling: Comptes Rendus Mécanique, Vol. 343, (2015): 38-56.
[13] S. Das, S. Chakraborty, R. N. Jana, O. D. Makinde, Entropy analysis of unsteady magneto-nanofluid flow past accelerating stretching sheet with convective boundary conditions. Applied Mathematics and Mechanics. Vol 36, (2015):1593-1610.
[14] S. O. Adesanya, O. D. Makinde, Irreversibility analysis in a couple stress film flow along an inclined heated plate with adiabatic free surface. Phys A,432 (2015): 222-229.
[15] S. O. Adesanya, O. D. Makinde, Entropy generation in couple stress fluid flow through porous channel with fluid slippage. International Journal of Energy 15,(2014): 344-362.

[16] S. Das, A.S. Banu, R.N. Jana, O.D. Makinde, Entropy analysis on MHD pseudo- plastic nanofluid flow through a vertical porous channel with convective heating, Alexandria Engineering Journal, Vol. 54(3), (2015):325-337.
[17] C. C. Cho, Heat transfer and entropy generation of natural convection in Nanofluid filled square cavity with partially-heated wavy surface, International Journal of Heat & Mass Transfer 77 (4), (2014): 818-827.
[18] K. Y. Leong, R. Saidur, M. Khairulmaini, Heat transfer and entropy analysis of three different types of heat exchangers operated with nanofluids. International Communications in Heat & Mass Transfer 39 (6), (2012): 838-843.
[19] A. H. Mahmoudi, I. Pop, M. Shahi, F. Talebi, MHD natural convection and entropy generation in a trapezoidal enclosure using Cu–water nanofluid. Computers & Fluids 72 (2013): 46–62.
[20] H. C. Brinkman, The viscosity of concentrated suspensions and solutions. J. Chem. Phys. 20 (1952): 571–581.
[21] J. C. Maxwell, A treatise on electricity and magnetism. 2nd ed. Cambridge: Oxford University Press; (1904): 435–441.
[22] S.J. Liao, The proposed homotopy analysis technique for the solution of non-linear problems Ph.D. Thesis, Shanghai Jiao Tong University, 1992.
[23] P.J. Hilton, An introduction to homotopy theory. Cambridge university press.(1953)
[24] J.C. Alexander and J.A. Yorke, The homotopy continuation method: numerically Implementable topological procedures. Trans. An. Math. Soc. 242,(1978) 271-284.
[25] T.F.C. Chan and H.B. Keller, arc-length continuation and muilti-grid techniques for nonlinear elliptic eigen values problems 978 SIAM J,sci.statist, comput.3,173-193.
[26] N. Dinar and H.B. keller, computations of taylor vortex flows using mulitigrid continuation methods tech rep. California Institute of technology. (1985)
[27] E.E. Grigolyuk and V.I, Shalashilin, problems of nonlinear deformation: the Continuation method applied to nonlinear problems in solid mechanics kluwer.(1991)
[28] S.J. Liao, An approximate solution technique which does not depend upon small parameters: a special example, Int. J. Non-Linear Mech. 30.
[29] S.J. Liao, Beyond perturbation introduction to the Homotopy analysis method, 1st edn, Chapman and Hall, CRC Press, Boca Ration 67.
[30] S.J. Liao,On the Homotopy analysis method for nonlinear problems, Appl.Math.Comput.,147 (2004): 499-513.
[31] S.J. Liao, An optimal Homotopy-analysis approach for strongly nonlinear differential equations, Common. Nonlinear Sci. Nume.Simulat., 15(2010): 2003-2016.
[32] S.J. Liao, The Homotopy analysis method in nonlinear differential equations, Springer and Higher education press,2012.
[33] S.J. Liao, An analytic approximation of the drag coefficient for the viscous flow past a sphere .Int. J. Non-Linear Mech. 37. (2002):1-18.

Appendix A

Approximate analytical expressions of the non-linear differential eqns. (7) and (8) using Homotopy analysis method

In this section, we indicate how the eqns. 17) and (18) are derived in this paper.
To find the solution of the equation (3.7) and (3.8) and reduced to

$$\frac{d^2w}{dy^2} - A2\,\mathrm{Re}\frac{dw}{dy} - A1\,Ha^2\,w + A3\,Gr\,\theta + Q\,L = 0 \qquad \text{(B.1)}$$

$$\frac{d^2\theta}{dy^2} - A6\,\mathrm{Pr}\,\mathrm{Re}\frac{d\theta}{dy} + A4\,Ec\,\mathrm{Pr}\left(\frac{dw}{dy}\right)^2 + A5\,Ec\,\mathrm{Pr}\,Ha^2\,w^2 = 0 \qquad \text{(B.2)}$$

We construct the HAM for (B.1) and (B.2) are as follows:

$$(1-p)\left(\frac{d^2w}{dy^2} + QL\right) - hp\left(\frac{d^2w}{dy^2} - A2\,\mathrm{Re}\frac{dw}{dy} - A1\,Ha^2\,w + A3\,Gr\,\theta + QL\right) = 0 \qquad \text{(B.3)}$$

$$(1-p)\left(\frac{d^2\theta}{dy^2} - A6\,\mathrm{Pr}\,\mathrm{Re}\frac{d\theta}{dy}\right) - hp\left(\begin{array}{l}\dfrac{d^2\theta}{dy^2} - A6\,\mathrm{Pr}\,\mathrm{Re}\dfrac{d\theta}{dy} + A4\,Ec\,\mathrm{Pr}\left(\dfrac{dw}{dy}\right)^2 \\ + A5\,Ec\,\mathrm{Pr}\,Ha^2\,w^2\end{array}\right) = 0 \qquad \text{(B.4)}$$

The approximate solution of the equation (B.3) and (B.4) are as follows:

$$w = w_0 + pw_1 + p^2w_2 + p^3w_3 + p^4w_4 + \ldots \qquad \text{(B.5)}$$

$$\theta = \theta_0 + p\theta_1 + p^2\theta_2 + p^3\theta_3 + p^4\theta_4 + \ldots \qquad \text{(B.6)}$$

Substituting the eqns.(B.5) into an eqn. (B.6), we get the following results:

$$\begin{array}{l}(1-p)\left(\dfrac{d^2(w_0 + pw_1 + \ldots)}{dy^2} + QL\right) \\ -h\,p\left(\begin{array}{l}\dfrac{d^2(w_0 + pw_1 + \ldots)}{dy^2} - A2\,\mathrm{Re}\dfrac{d(w_0 + pw_1 + \ldots)}{dy} \\ - A1\,Ha^2(w_0 + pw_1 + \ldots) + A3\,Gr(\theta_0 + p\theta_1 + \ldots) + QL\end{array}\right) = 0\end{array} \qquad \text{(B.7)}$$

$$\begin{array}{l}(1-p)\left(\dfrac{d^2(\theta_0 + p\theta_1 + \ldots)}{dy^2} - A6\,\mathrm{Pr}\,\mathrm{Re}\dfrac{d(\theta_0 + p\theta_1 + \ldots)}{dy}\right) \\ -h\,p\left(\begin{array}{l}\dfrac{d^2(\theta_0 + p\theta_1 + \ldots)}{dy^2} - A6\,\mathrm{Pr}\,\mathrm{Re}\dfrac{d(\theta_0 + p\theta_1 + \ldots)}{dy} \\ + A4\,Ec\,\mathrm{Pr}\left(\dfrac{d(w_0 + pw_1 + \ldots)}{dy}\right)^2 \\ + A5\,Ec\,\mathrm{Pr}\,Ha^2(w_0 + pw_1 + \ldots)^2\end{array}\right) = 0\end{array} \qquad \text{(B.8)}$$

Comparing the coefficients of like powers of p^0, p^1 in the eqns. (B.7) and (B.8) we get

$$p^0 : \frac{d^2w_0}{dy^2} + QL = 0 \qquad \text{(B.9)}$$

$$p^0 : \frac{d^2\theta_0}{dy^2} - A6\ \mathrm{Pr}\,\mathrm{Re}\frac{d\theta_0}{dy} = 0 \qquad \text{(B.10)}$$

$$P^1 : \frac{d^2 w_1}{dy^2} - \frac{d^2 w_0}{dy^2} - QL - h\left(\frac{d^2 w_0}{dy^2} - A2\,\mathrm{Re}\frac{dw_0}{dy} - A1\,Ha^2 w_0 + A3\,Gr\,\theta_0 + QL \right) = 0 \qquad \text{(B.11)}$$

$$P^1 : \frac{d^2 \theta_1}{dy^2} - A6\,\mathrm{Pr}\,\mathrm{Re}\frac{d\theta_1}{dy} - \frac{d^2 \theta_0}{dy^2} + A6\,\mathrm{Pr}\,\mathrm{Re}\frac{d\theta_0}{dy} - h\begin{pmatrix} \frac{d^2 \theta_0}{dy^2} - A6\,\mathrm{Pr}\,\mathrm{Re}\frac{d\theta_0}{dy} \\ + A4\,Ec\,\mathrm{Pr}\left(\frac{dw_0}{dy}\right)^2 \\ + A5\,Ec\,\mathrm{Pr}\,Ha^2 {w_0}^2 \end{pmatrix} = 0 \qquad \text{(B.12)}$$

The initial approximations are as follows:

$$w_0(0) = 0\ ,\ \theta_0(0) = 0$$
$$w_0(1) = 0\ ,\ \theta_0(1) = 1 \qquad \text{(B.13)}$$
$$w_j(0) = 0\ ,\ \theta_j(0) = 0$$
$$w_j(1) = 0\ ,\ \theta_j(1) = 0,\ \ j = 1,2,3,..... \qquad \text{(B.14)}$$

Solving the eqns. (B.9) - (B.12) and using the initial approximations (B.13) and (B.14), we can obtain the following results:

$$w_0 = \frac{QLA1A2A3Gr}{2}\left(y - y^2\right) \qquad \text{(B.15)}$$

$$w_1 = -h\begin{bmatrix} \frac{QLA1A2^2A3Gr\,\mathrm{Re}}{2}\left(\frac{y^2}{2} - \frac{y^3}{3}\right) \\ + \frac{QLA1^2A2A3Gr\,Ha^2}{2}\left(\frac{y^3}{6} - \frac{y^4}{12}\right) \\ -\left(\frac{-1}{2}\frac{y^2}{e^f - 1} + \frac{e^{f,y}}{f^2\left(e^f - 1\right)}\right) - \frac{QLy^2}{2} \\ + t_1 y + t_2 \end{bmatrix} \qquad \text{(B.16)}$$

$$\theta_0 = C_1 + C_2 e^{f.y} \qquad \text{(B.17)}$$

$$\theta_1 = -h\begin{bmatrix} \frac{e^{f.y}}{A4\,A5\,Ec\left(e^f - 1\right)} - \frac{A1^2A2^2A3^2A4\,Ec\,\mathrm{Pr}\,Q^2L^2Gr^2}{192}\left(1 - 2y^4\right) \\ - \frac{A1^2A2^2A3^2A5\,Ec\,\mathrm{Pr}\,Q^2L^2Gr^2Ha^2}{4}\left(\frac{y^6}{30} - \frac{y^5}{10} + \frac{y^4}{12}\right) \\ + t_3 y + t_4 \end{bmatrix} \qquad \text{(B.18)}$$

where f, t_1, t_2, t_3, t_4 are defined in the eqns.(7)-(21) respectively.

According to HAM, we can conclude that

$$w = \lim_{P \to 1} w(\eta) = w_0 + w_1 \qquad \text{(B.19)}$$

$$\theta = \lim_{P \to 1} \theta(\eta) = \theta_0 + \theta_1 \qquad \text{(B.20)}$$

After putting the eqns. (B.15) and (B.16) into an eqn.(B.19) and putting the eqns.(B.17) and (B.18) into an eqns.(B.20), we can obtain the solution in text eqns. (17) and (18).

Appendix: B – Nomenclature

Symbol	Meaning
u, v	Velocities of the fluid
ρ	Fluid density
p	Fluid pressure
x, y	Coordinates
L	axial pressure gradient parameter
T_0	Temperature at the lower plate
T_1	Temperature at upper plate
T	Fluid temperature
μ	Coefficient of viscosity
Pr	Prandtl number
Ha	Hartmann number
Gr	Grashof number
Be	Bejan number
N_s	Entropy generation rate
θ	Dimensionless temperature
Re	Reynolds number
Ec	Eckert number
Pe	Peclet number
Br	Brinkmann number
Ω	Temperature difference parameter
y	Dimensionless transverse coordinate
ϕ	Irreversibility ratio